Supporting Information for

Exclusive occurrence of photoinduced energy transfer and switching its direction by rectangular π-extension of nanographenes

Tomokazu Umeyama,*[a] Takuma Hanaoka,[a] Hiroki Yamada,[a] Yuki Namura,[a]
Satoshi Mizuno,[a] Tomoya Ohara,[a] Jinseok Baek,[a] JaeHong Park,[a] Yuta Takano,[b]
Kati Stranius,[c] Nikolai V. Tkachenko,*[c] and Hiroshi Imahori*[ab]

[a] *Department of Molecular Engineering, Graduate School of Engineering, Kyoto University, Nishikyo-ku, Kyoto, 615-8510, Japan*

[b] *Institute for Integrated Cell-Material Sciences (WPI-iCeMS), Kyoto University, Sakyo-ku, Kyoto 606-8501, Japan*

[c] *Department of Chemistry and Bioengineering, Tampere University of Technology, P.O. Box 541, FIN-33101 Tampere, Finland*

E-mail: umeyama@scl.kyoto-u.ac.jp, nikolai.tkachenko@tuni.fi, imahori@scl.kyoto-u.ac.jp

Experimental

Materials

All solvents and chemicals were of reagent grade quality, purchased, and used without further purification. 1,4-Diiodo-2,3,5,6-tertakis(*p*-(3,7-dimethyloctyl)phenyl)benzene (TPB-I), 1,4-bis(*p*-pinacolatoborylphenyl)-2,3,5,6-tertakis(*p*-(3,7-dimethyloctyl)phenyl)benzene (pinB-HPB), 5-(*p*-bromophenyl)-10,15,20-tris(3,5-di-*tert*-butylphenyl)-porphyrinatozinc(II) (ZnP-Br) were prepared according to the reported procedures.[S1,S2]

Synthesis

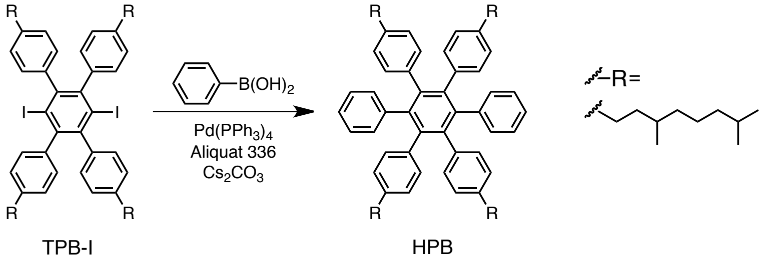

1,4-Diphenyl-2,3,5,6-tertakis(*p*-(3,7-dimethyloctyl)phenyl)benzene (HPB). To TPB-I (366 mg, 0.306 mmol) and phenylboronic acid (219 mg, 1.84 mmol) in toluene (8 mL) were added $Pd(PPh_3)_4$ (18 mg, 0.016 mmol), *N*-methyl-*N*,*N*,*N*-trioctylammonium chloride (Aliqat 336, 0.4 mg, 1×10^{-3} mmol) and Cs_2CO_3 (995 mg, 3.06 mmol) under argon atmosphere. The reaction mixture was heated at 100˚C with stirring for 24 h. The mixture was washed with water, extracted with dichloromethane and dried with $MgSO_4$. Then, solvent was removed under vacuum and the solid residue was purified by column chromatography (SiO_2, dichloromethane : hexane = 1 : 20), yielding HPB as viscous oil (285 mg, 0.260 mmol, 85%). ^{1}H NMR (400 MHz, $CDCl_3$) δ 6.81 (s, 10H), 6.68-6.62 (m, 16H), 2.42-2.29 (m, 8H), 1.56-0.69 (m, 76H). ^{13}C NMR (75.45 MHz, $CDCl_3$) δ: 141.2, 140.4, 139.6, 138.2, 131.7, 131.5, 130.8, 130.5, 127.2, 126.5, 39.5, 38.7, 37.2, 33.0, 32.2, 28.0, 24.7, 22.6, 19.7. IR (ATR): 2954, 2926, 2869, 1514, 1463, 1380, 836, 700 cm^{-1}. HRMS (MALDI-TOFMS, m/z) = 1095.8662 (M + H$^+$); calcd for $C_{82}H_{110}$: 1094.8607.

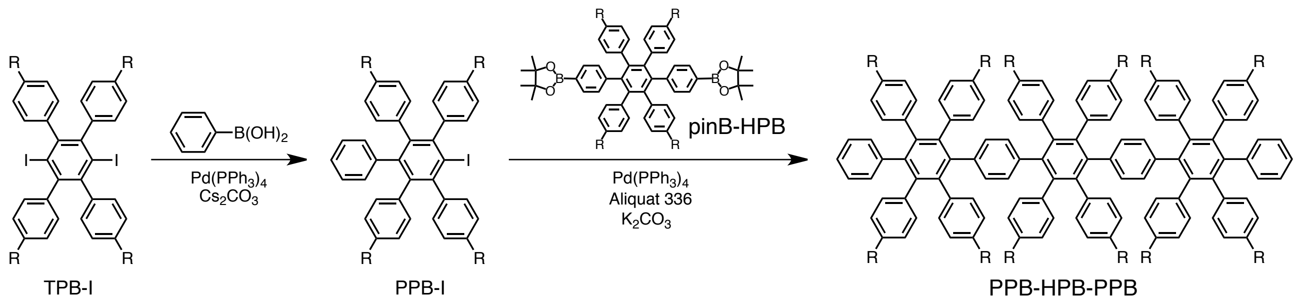

1-Iodo-4-phenyl-2,3,5,6-tertakis(*p*-(3,7-dimethyloctyl)phenyl)benzene (PPB-I). To TPB-I (496 mg, 0.415 mmol) and phenylboronic acid (76 mg, 0.622 mmol) in toluene (13 mL) were added Pd(PPh$_3$)$_4$ (23 mg, 0.020 mmol) and Cs$_2$CO$_3$ (1.35 g, 4.15 mmol) under argon atmosphere. The reaction mixture was heated at 80˚C with stirring for 24 h. The mixture was washed with water, extracted with dichloromethane and dried with MgSO$_4$. Then, solvent was removed under vacuum and the solid residue was purified by column chromatography (SiO$_2$, dichloromethane:hexane = 1:20), yielding PPB-I as viscous oil (101 mg, 8.83 × 10^{-2} mmol, 21%). ^{1}H NMR (400 MHz, CDCl$_3$) δ 6.97 (s, 9H), 6.77 (s, 5H), 6.67-6.60 (m, 7H), 2.53-2.48 (m, 4H), 2.39-2.28 (m, 4H), 1.53-0.71 (m, 76H). ^{13}C NMR (75.45 MHz, CDCl$_3$) δ: 146.1, 143.2, 141.2, 141.3, 141.2, 140.2, 140.0, 138.0, 131.2, 131.1, 131.0, 130.4, 127.1, 126.5, 126.4, 125.1, 39.5, 38.7, 38.6, 37.3, 33.3, 32.9, 32.5, 32.2, 28.0, 24.7, 22.7, 22.6, 19.7, 19.6. IR (ATR): 2956, 2924, 2865, 1515, 1464, 1382, 1023, 829, 700 cm^{-1}. HRMS (MALDI-TOFMS, m/z) = 1144.7246 (M$^{\bullet+}$); calcd for $C_{76}H_{105}I$: 1144.7261.

PPB-HPB-PPB. To PPB-I (113 mg, 9.89 × 10^{-2} mmol) and pinB-HPB (68.7 mg, 5.10 × 10^{-2} mmol) in toluene (3 mL) and H$_2$O (1.1 mL) were added Aliqat 336 (0.4 mg, 1 × 10^{-3} mmol) and K$_2$CO$_3$ (152 mg, 1.09 mmol) under argon atmosphere. This mixture was then degassed by three freeze-pump-thaw cycles and refilled with argon. Then, Pd(PPh$_3$)$_4$ (5.8 mg, 5.0 × 10^{-2} mmol) was added quickly and the reaction mixture was degassed three times again via freeze-pump-thaw cycles. The reaction mixture was refluxed with stirring for 48 h. The mixture was washed with water, extracted with dichloromethane and dried with MgSO$_4$. Then, solvent was removed under vacuum and the solid residue was purified by column chromatography (SiO$_2$, dichloromethane:hexane = 1:20) and gel permeation chromatography (chloroform), yielding PPB-HPB-PPB as viscous oil (58.3 mg, 1.86 × 10^{-2} mmol, 38%). ^{1}H NMR (300 MHz, CDCl$_3$) δ 6.78 (s, 8H), 6.69 (s, 18H), 6.58 (s, 16H), 6.51 (s, 8H), 6.45 (s, 8H), 6.17-6.12 (m, 8H), 2.43 (m, 24H), 1.54-0.80 (m, 228H). ^{13}C NMR (75.45 MHz, $CDCl_3$) δ: 141.3, 140.6, 140.4, 140.3, 139.7, 139.5, 139.4, 139.3, 138.6, 138.4, 137.0, 136.8, 131.9, 131.8, 131.5, 130.4, 126.4, 124.7, 39.5, 38.9, 38.7, 37.3, 33.1, 33.0, 32.4, 32.1, 28.0, 24.7, 22.7, 22.6, 19.7, 19.6. IR (ATR): 2958, 2927, 2868, 1514, 1469, 1383, 1022, 853, 830, 700 cm^{-1}. HRMS (APCI-MS, m/z) = 3128.4850 ($M^{\bullet+}$); calcd for $C_{234}H_{318}$: 3128.4883.

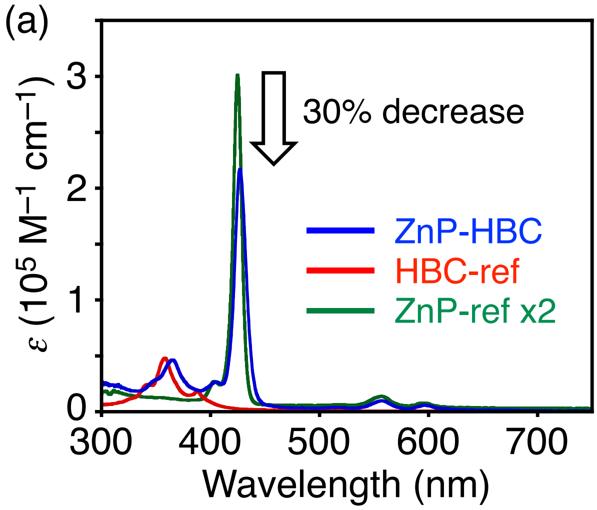

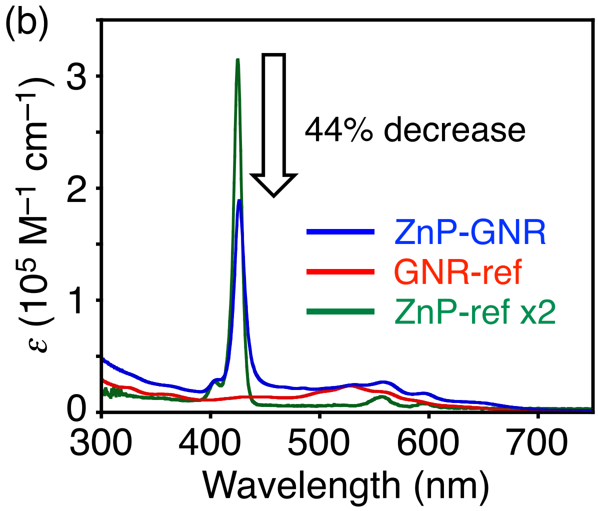

Fig. S1 UV-visible absorption spectra of (a) ZnP-HBC (blue), HBC-ref (red), and ZnP-ref (green) and (b) ZnP-GNR (blue), GNR-ref (red), and ZnP-ref (green) in THF. The absorption intensity of ZnP-ref is doubled, reflecting that the two ZnP units are present in ZnP-HBC and ZnP-GNR. Diminution rates of the Soret band absorption intensities of ZnP-HBC and ZnP-GNR with respect to ZnP-ref at the maxima are shown in figures.

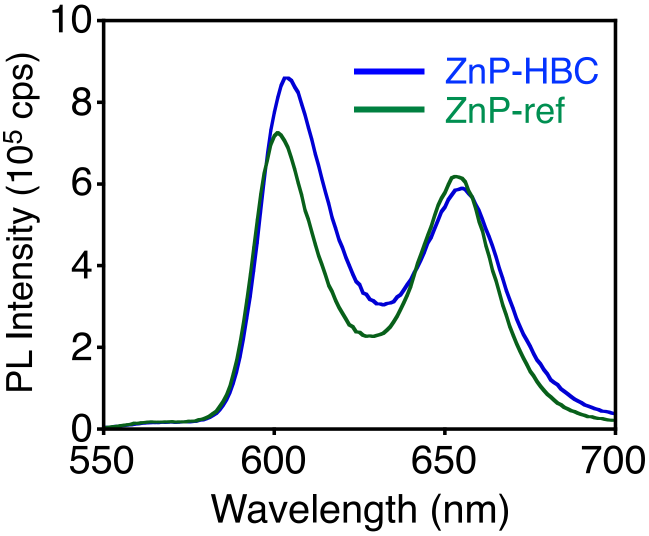

Fig. S2 Fluorescence spectra of ZnP-HBC (blue) and ZnP-ref (green) in THF. The excitation wavelength is 426 nm, where the absorbances are adjusted to be identical for comparison.

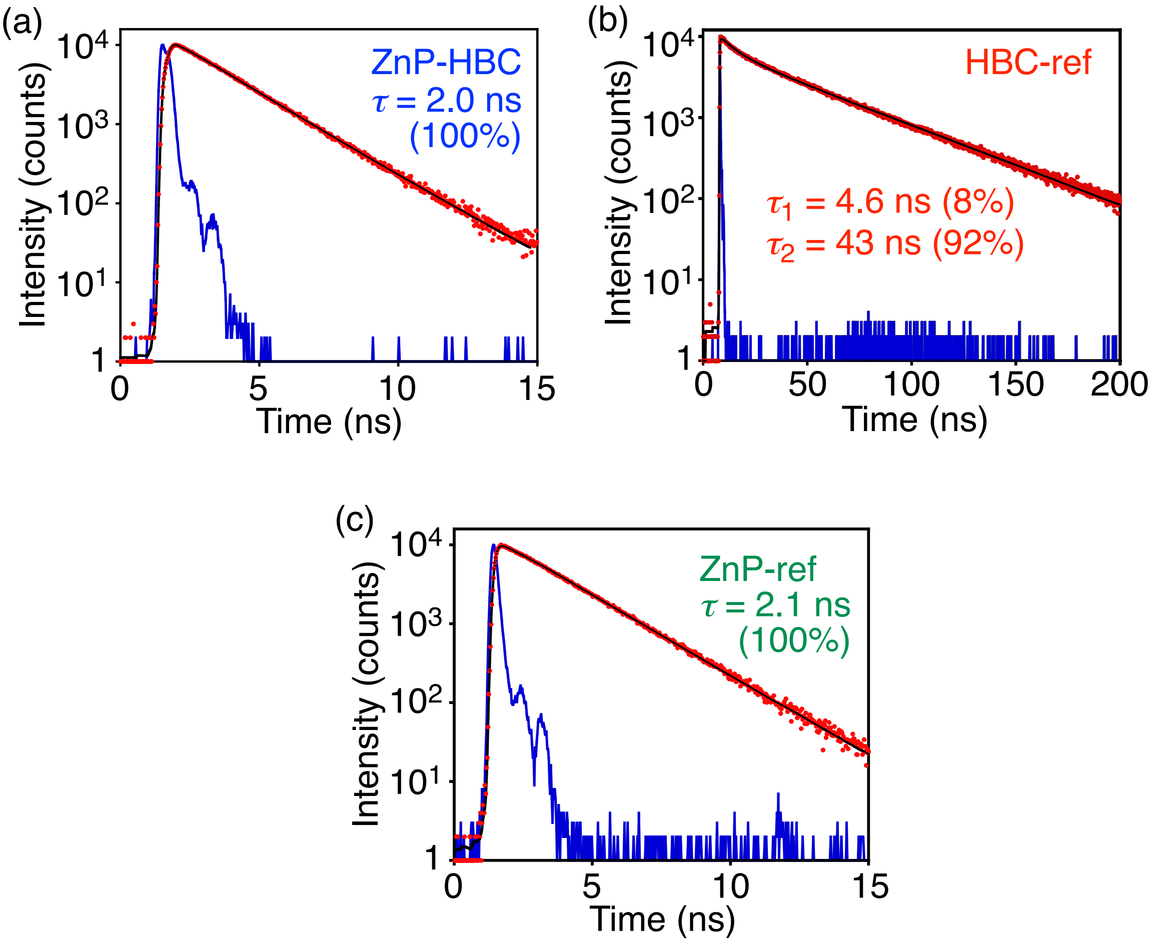

Fig. S3 Nanosecond fluorescence decays (red), decay fittings (black), and instrumental response functions (blue) of (a) ZnP-HBC, (b) HBC-ref, and (c) ZnP-ref measured in THF by TCSPC technique. The excitation wavelengths are 378 nm, 378 nm, 416 nm, respectively. The emission detection wavelengths are 650 nm, 500 nm and 650 nm, respectively. The fluorescence lifetimes (τ) with the ratios are given in the figures. The fluorescence lifetimes of HBC-ref and ZnP-ref agree with the values reported in literatures.[S2,S3] The existence of the two decay components in HBC-ref may stem from two emitting species, i.e., whole graphene and edge structures.[S4]

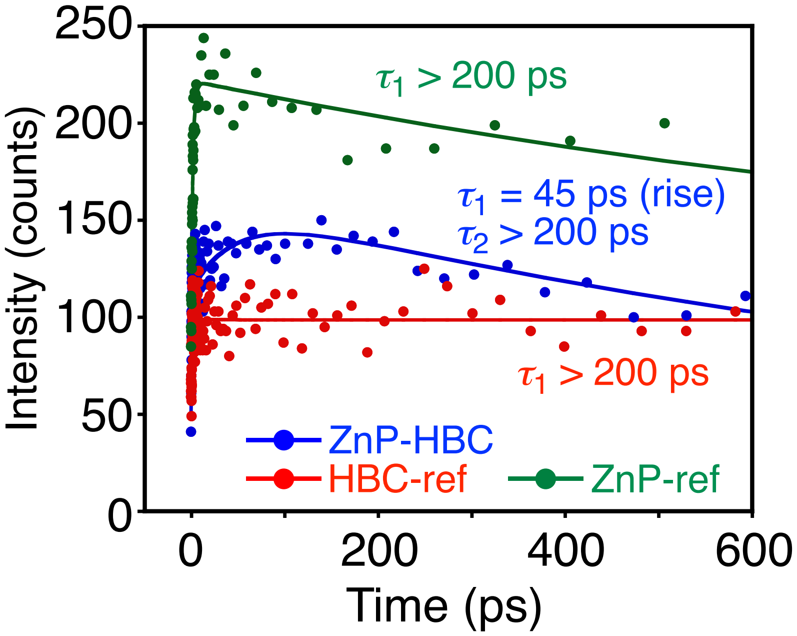

Fig. S4 Picosecond fluorescence decays of ZnP-HBC (blue), HBC-ref (red), and ZnP-ref (green) measured in THF by a photon up-conversion technique. The excitation wavelengths are 405 nm for all samples. The emission detection wavelengths are 650 nm, 550 nm and 650 nm, respectively. The solid lines present decay fittings and the fluorescence lifetimes (τ) are given in the figures. The τ_2 value of ZnP-HBC, τ_1 value of HBC-ref, and τ_1 value of ZnP-ref exceed the detection limit of the measurement system (200 ps).

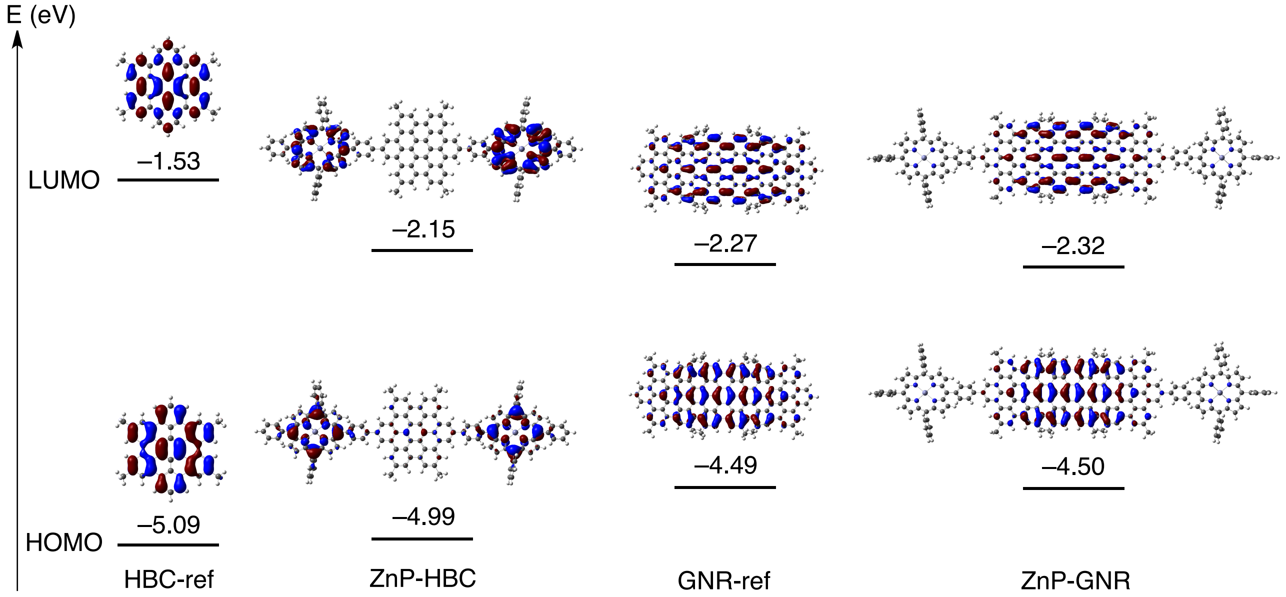

Fig. S5 Optimized geometries, HOMO/LUMO electron density distributions, and energy levels of HBC-ref, ZnP-HBC, GNR-ref, and ZnP-GNR by DFT calculations using spin-restricted B3LYP/6-31G model. The long alkyl chains of HBC/GNR and 2,4,6-trimethylphenyl groups of ZnP are replaced with methyl and phenyl groups, respectively, to shorten the calculation time.

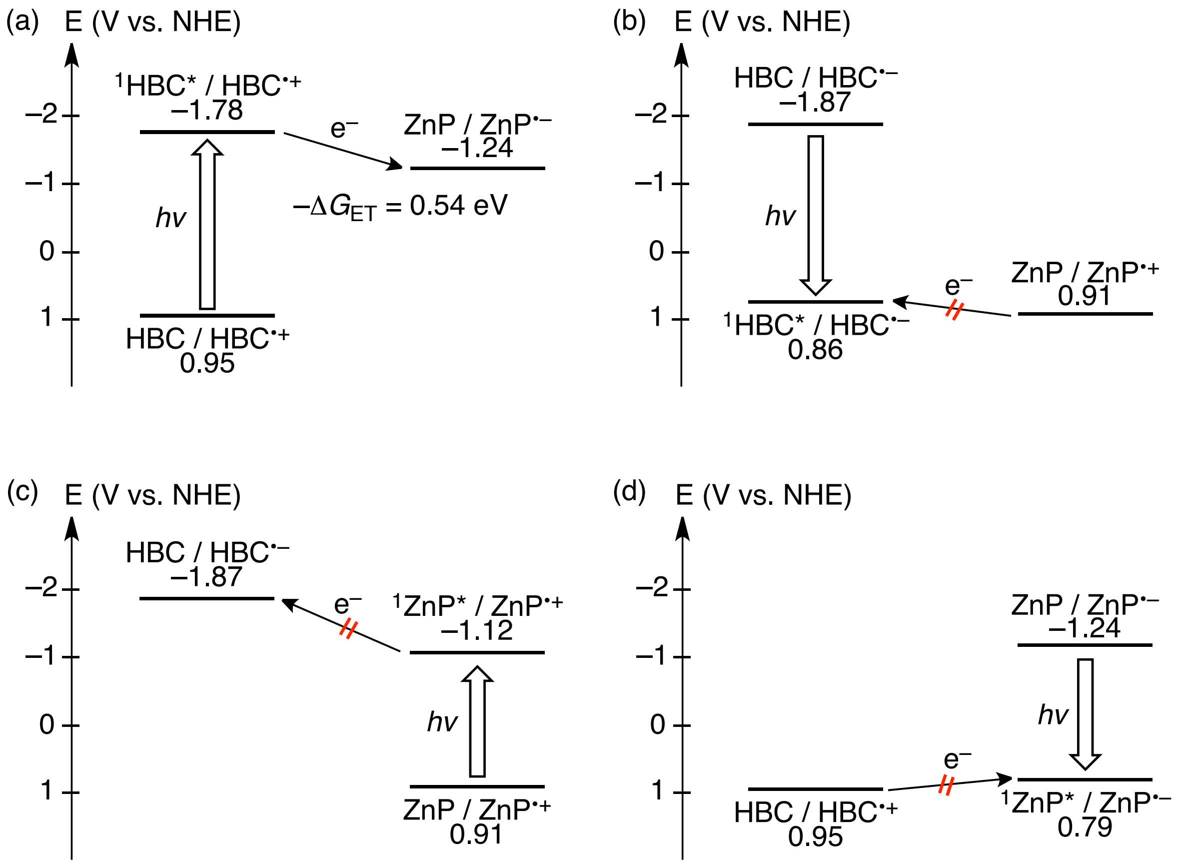

Fig. S6 Energy diagrams for electron transfer (ET) (a) from the singlet excited state of HBC (^{1}HBC*) to ZnP, (b) from ZnP to ^{1}HBC*, (c) from the singlet excited state of ZnP (^{1}ZnP*) to HBC, and (d) from HBC to ^{1}ZnP* in HBC-ZnP. The first oxidation and reduction potentials of HBC and ZnP moieties were determined by DPV measurements of HBC-ref and ZnP-ref. The optical bandgaps of HBC and ZnP moieties were estimated from the absorption edges of HBC-ref and ZnP-ref. ET is energetically favorable only from ^{1}HBC* to ZnP in (a). The driving force of ET ($-\Delta G_{\mathrm{ET}}$) in (a) was estimated to be 0.54 eV (= (the optical bandgap energy of HBC) – {(the first oxidation potential of HBC) – (the first reduction potential of ZnP)}).

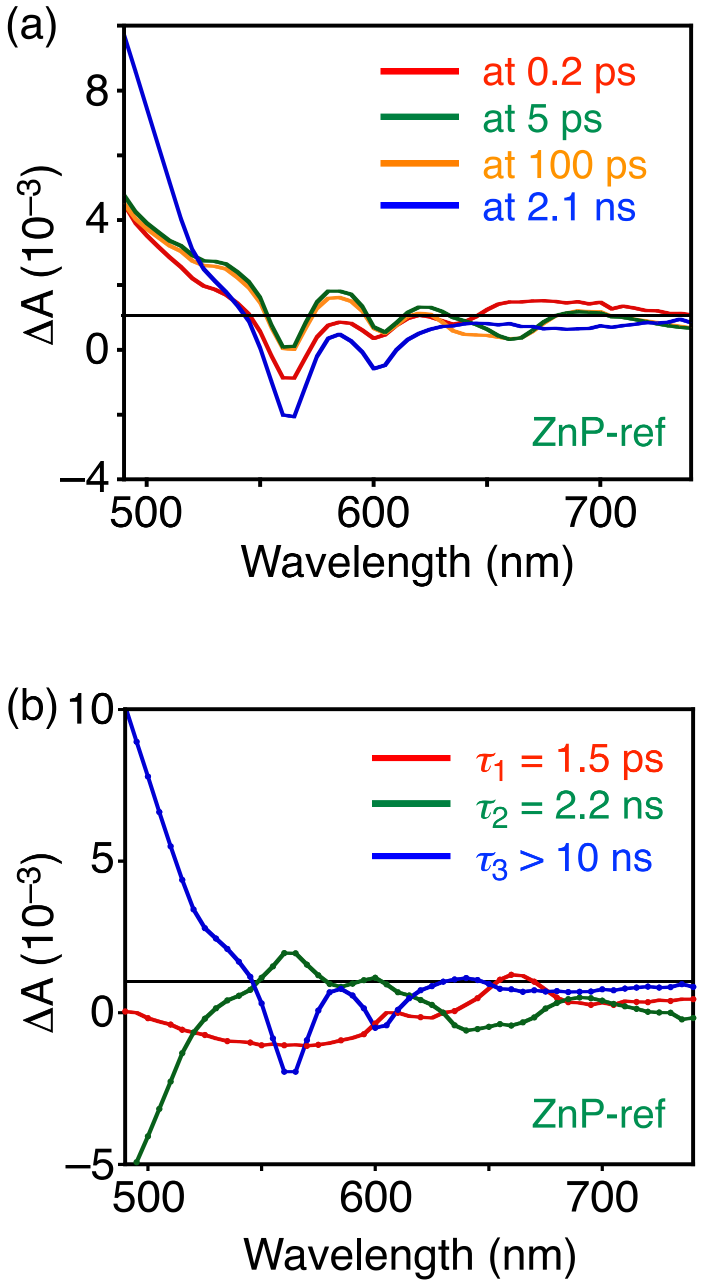

Fig. S7 (a) Femto- to picosecond time-resolved TA spectra of ZnP-ref excited at 360 nm in THF. The spectra at delay times of 0.2 ps-2.1 ns are shown. (b) Femto- to picosecond transient absorption decay component spectra of ZnP-ref in THF obtained with global three components fit of the data. Lifetimes of respective components are given in (b): the transition from the second (S_2) to first (S_1) singlet excited state of ZnP (τ_1 = 1.5 ps), the decay of the S_1 state of ^{1}ZnP* (τ_2 = 2.2 ns), and that of ^{3}ZnP* (τ_3 > 10 ns).

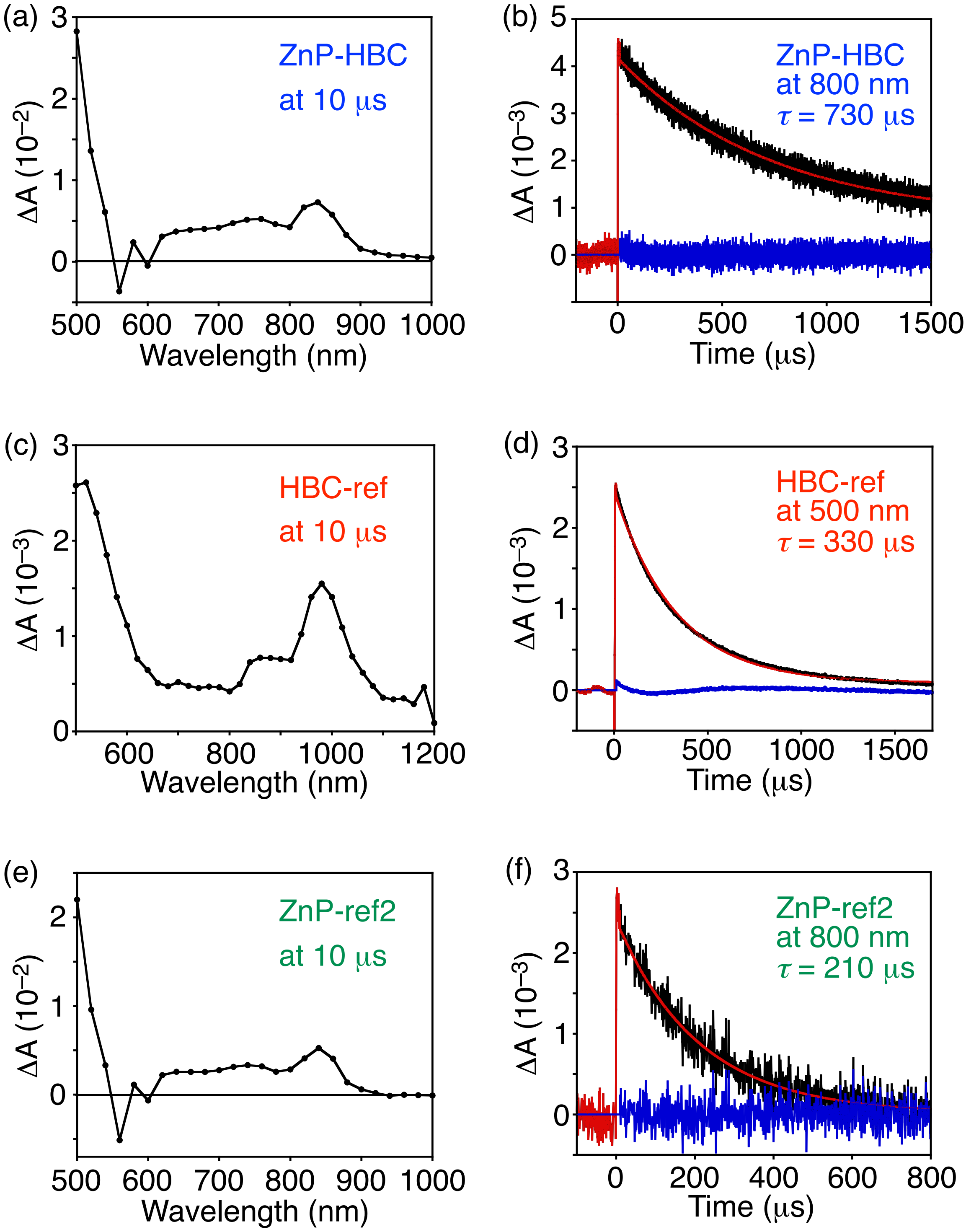

Fig. S8 Nano- to microsecond time-resolved TA spectra of (a) ZnP-HBC, (c) HBC-ref, and (e) ZnP-ref2 (5-phenyl-10,15,20-tris(3,5-di-*tert*-butylphenyl)-porphyrinatozinc(II))[S5] in THF at 10 μs after the photoexcitation. Excitation wavelengths are 360 nm, 360 nm, and 425 nm, respectively. Decay profiles (black), monoexponential fitting curves (red), and fitting residuals (blue) of (b) ZnP-HBC at 800 nm, (d) HBC-ref at 500 nm, and (f) ZnP-ref2 at 800 nm.

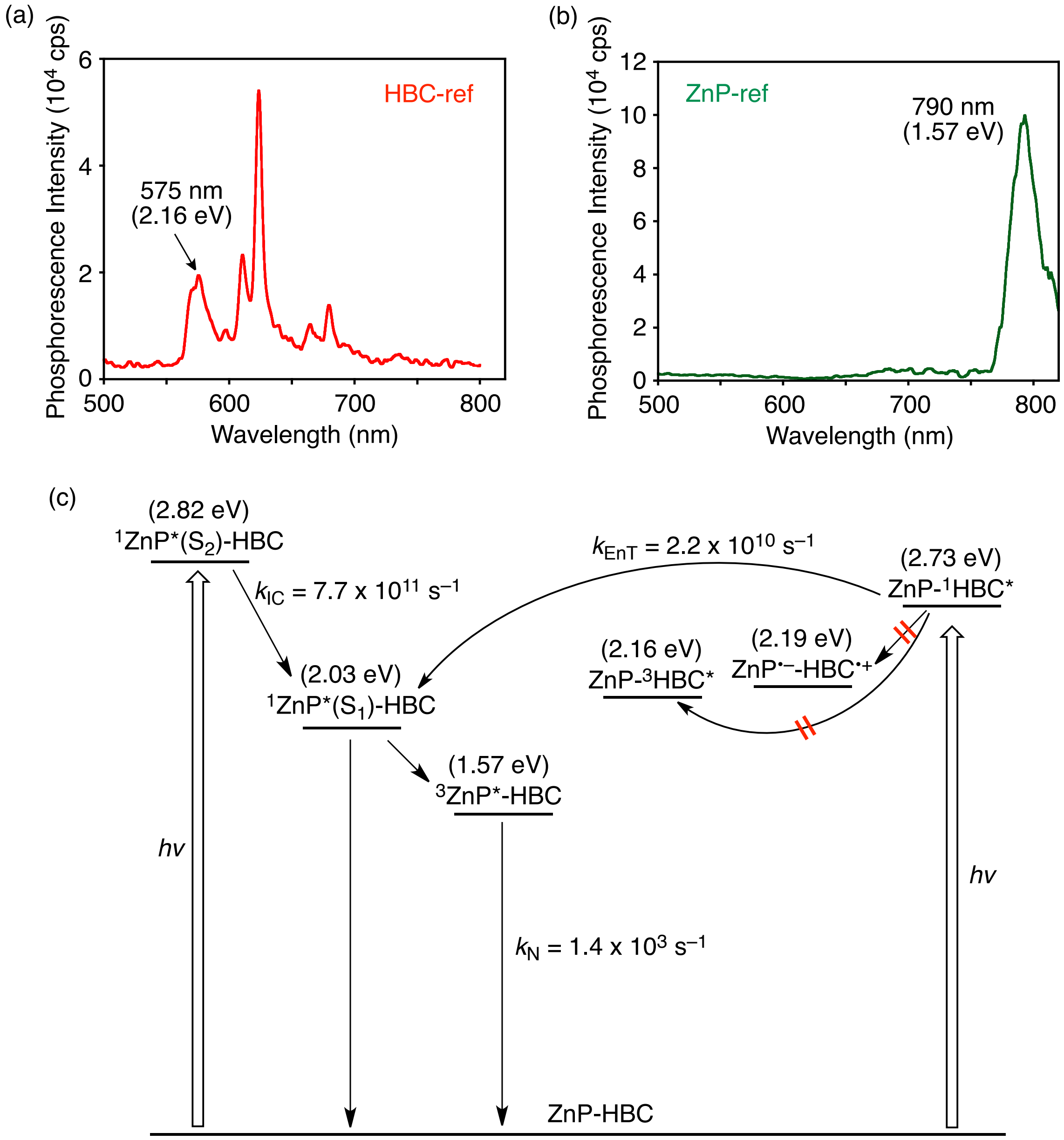

Fig. S9 Phosphorescence spectra of (a) HBC-ref and (b) ZnP-ref in 2-methyltetrahydrofuran at 77 K. The excitation wavelengths are 360 nm and 422 nm, respectively. The energy levels of ^{3}HBC* and ^{3}ZnP* were determined by the peak positions of the phosphorescence with the highest energies.[S6,S7] (c) Relaxation pathways of ZnP-HBC. The energy level of the S$_2$ state of ^{1}ZnP* was determined from the absorption edge of the Soret band of ZnP-ref.

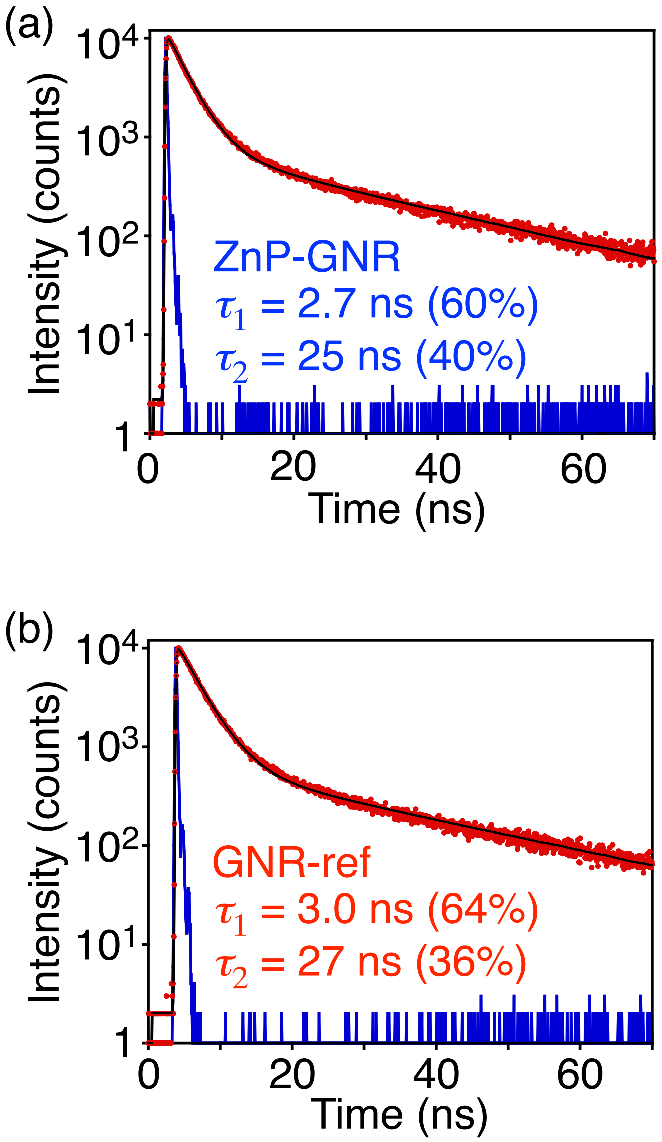

Fig. S10 Nanosecond fluorescence decays (red), decay fittings (black), and instrumental response functions (blue) of (a) ZnP-GNR and (b) GNR-ref excited at 416 nm in THF by TCSPC technique. The emission detection wavelength is 650 nm. The fluorescence lifetimes (τ) with the ratios are given in the figures. The existence of the two decay components in ZnP-GNR and GNR-ref may stem from two emitting species in the GNR core, i.e., whole graphene and edge structures.[S4]

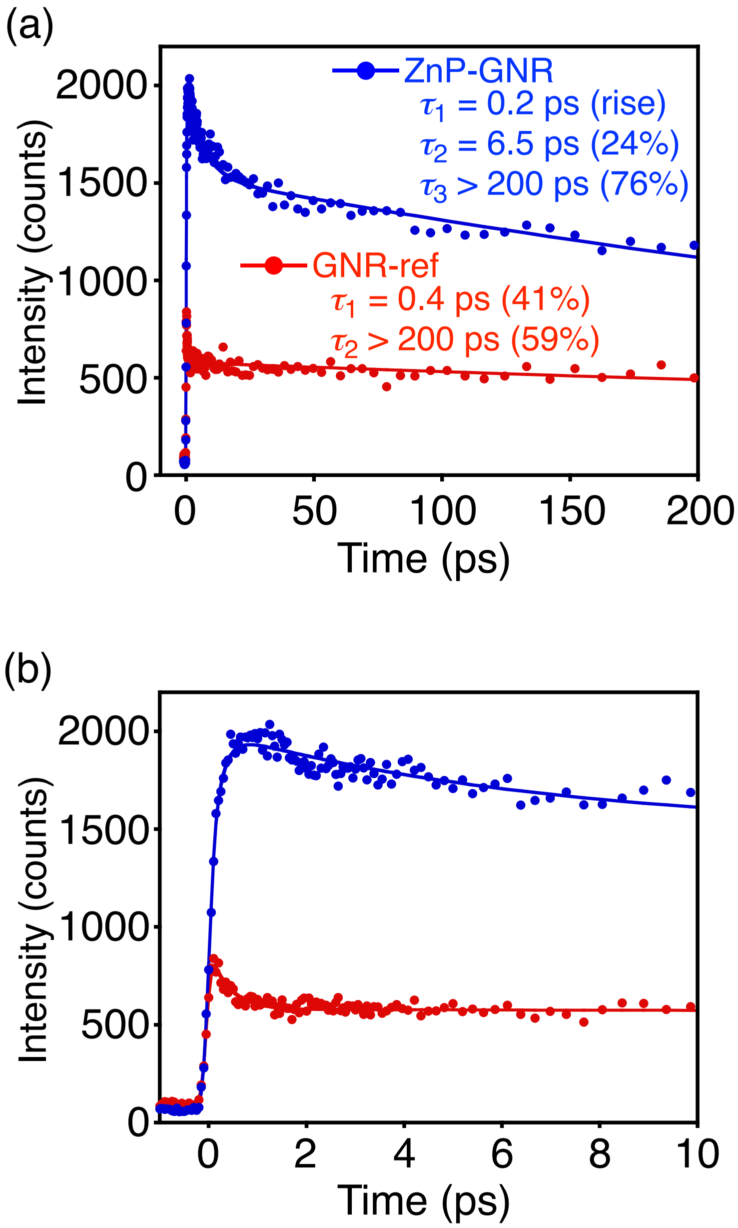

Fig. S11 (a) Picosecond fluorescence decays of ZnP-GNR (blue) and GNR-ref (red) measured in THF by a photon up-conversion technique. (b) Enlarged decay profiles. The excitation and emission detection wavelengths are 425 nm and 650 nm, respectively. The absorption ratio of ZnP and GNR is 6:1 in ZnP-GNR at 425 nm. The solid lines present decay fittings and the fluorescence lifetimes (τ) with the ratios are given in (a). The existence of the multiple decay components in GNR-ref may stem from multiple emitting species in the GNR core, i.e., whole graphene and edge structures.[S4] The first component of ZnP-GNR (rise, τ_1 = 0.2 ps) can be attributed to the energy transfer from the S_2 state of ^{1}ZnP* to GNR. The second component (decay, τ_2 = 6.5 ps) stems from the fluorescence from the S_1 state of ^{1}ZnP*, whereas the third component (decay, τ_3 > 200 ps) is derived from the excited singlet state of GNR.

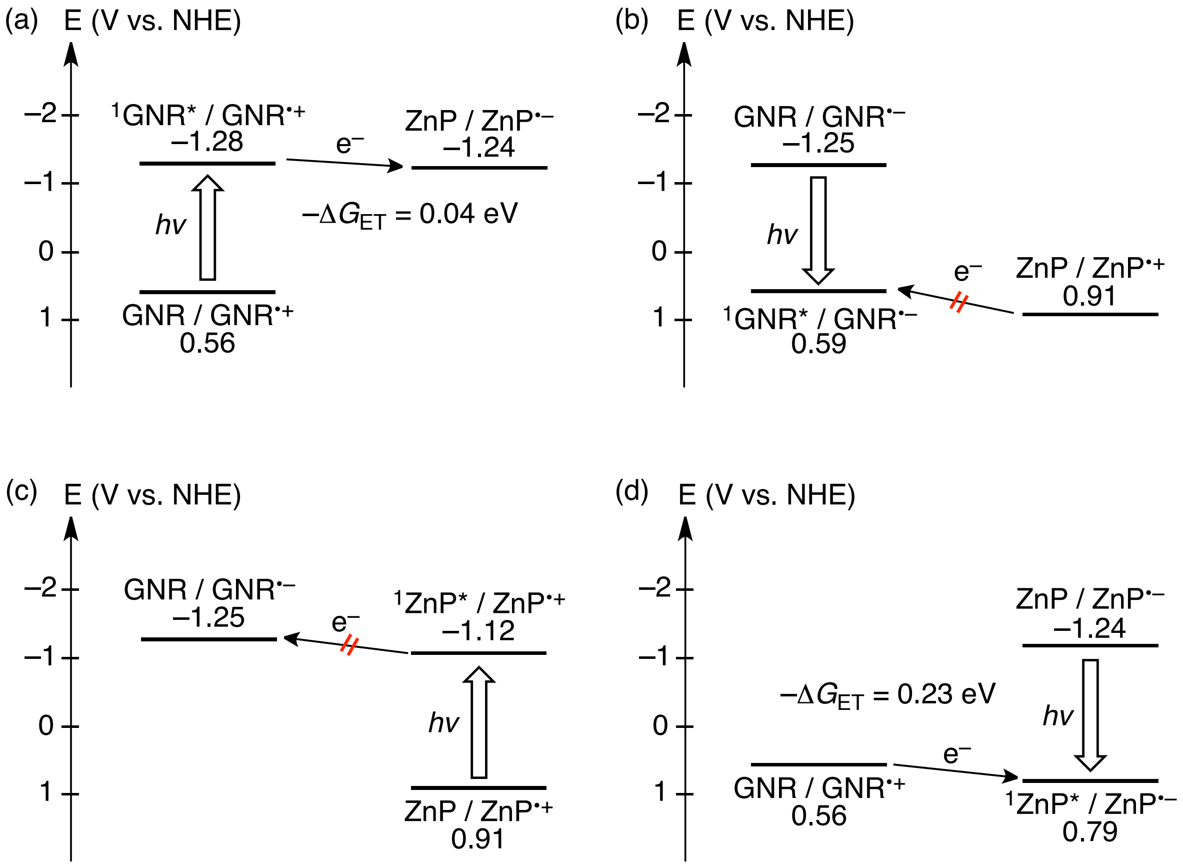

Fig. S12 Energy diagrams for ET (a) from the singlet excited state of GNR (^{1}GNR*) to ZnP, (b) from ZnP to ^{1}GNR*, (c) from the singlet excited ZnP (^{1}ZnP*) to GNR, and (d) from GNR to ^{1}ZnP* in ZnP-GNR. The first oxidation and reduction potentials of GNR and ZnP moieties were determined by DPV measurements of GNR-ref and ZnP-ref. The optical bandgaps of GNR and ZnP moieties were estimated from the absorption edges of GNR-ref and ZnP-ref. Electron transfers are energetically favorable only from ^{1}GNR* to ZnP in (a) and from GNR to ^{1}ZnP* in (d). The driving forces of ET ($-\Delta G_{\mathrm{ET}}$) were estimated to be 0.04 eV (= (the optical bandgap energy of GNR) – {(the first oxidation potential of GNR) – (the first reduction potential of ZnP)}) in (a) and 0.23 eV (= (the optical bandgap energy of ZnP) – {(the first oxidation potential of GNR) – (the first reduction potential of ZnP)}) in (d).

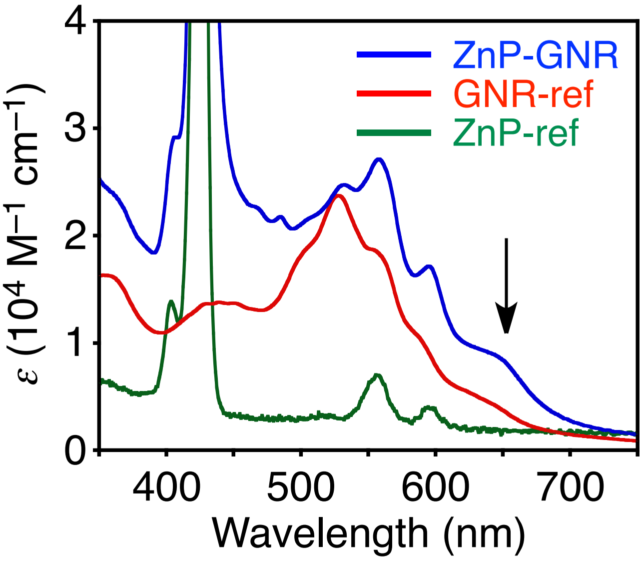

Fig. S13 UV-visible absorption spectra of ZnP-GNR (blue), GNR-ref (red), and ZnP-ref (green) in THF (enlarged spectra of Fig. 1b). The arrow marks the shoulder at 655 nm.

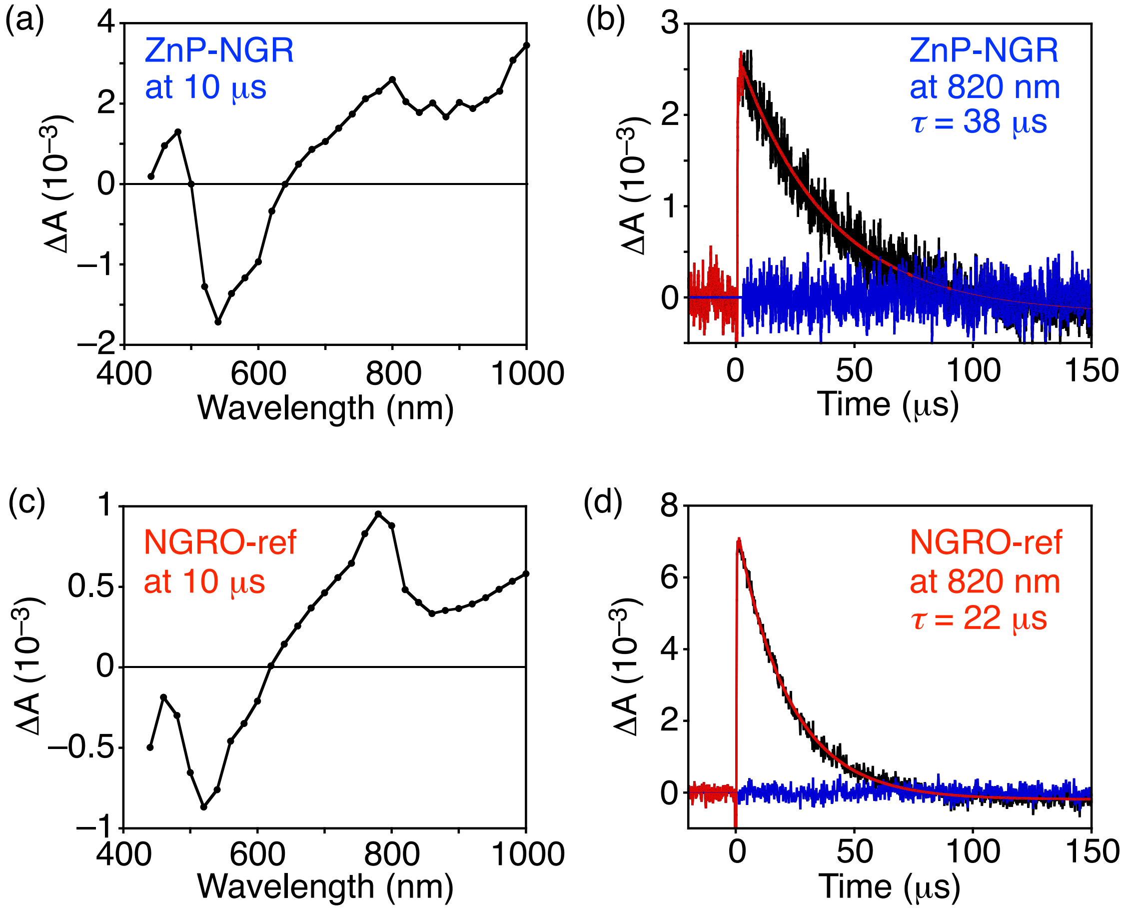

Fig. S14 Nano- to microsecond time-resolved TA spectra of (a) ZnP-GNR and (c) GNR-ref at 10 μs after the photoexcitation in THF. Excitation wavelengths are 425 nm. Decay profiles (black), monoexponential fitting curves (red), and fitting residuals (blue) of (b) ZnP-GNR and (d) GNR-ref at 820 nm.

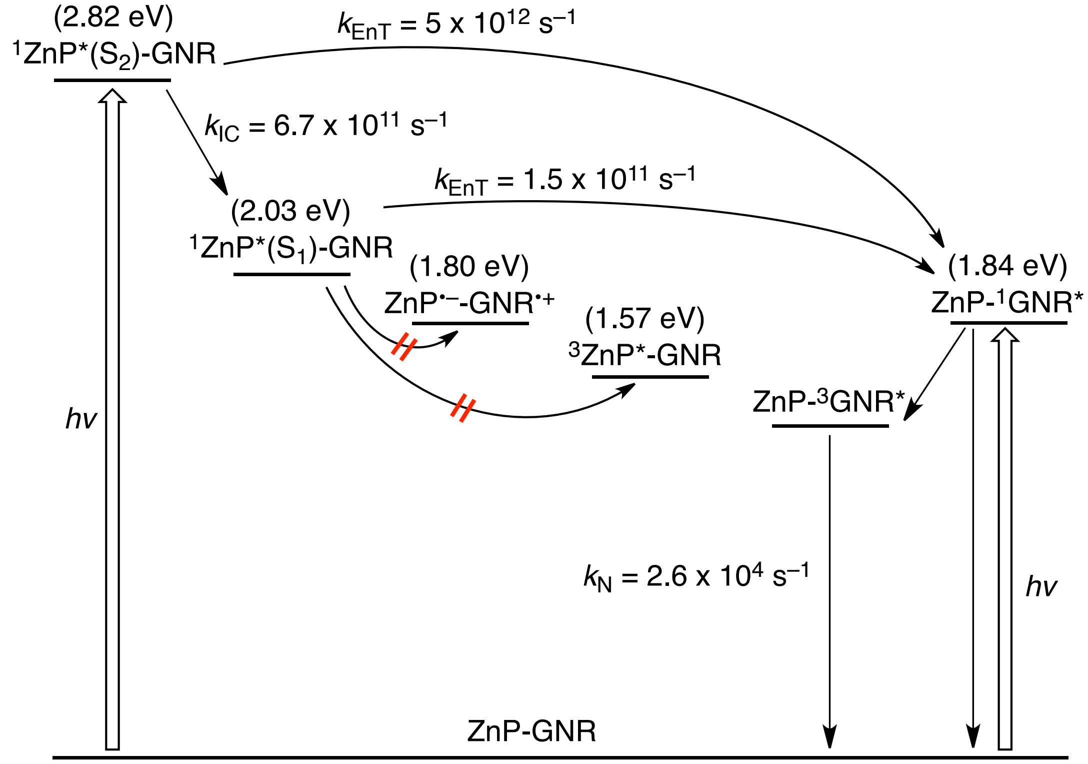

Fig. S15 Relaxation pathways of ZnP-GNR.

References

[S1] X. Yang, X. Dou, A. Rouhanipour, L. Zhi, J. H. Räder and K. Müllen, *J. Am. Chem. Soc.*, 2008*,* **130**, 4216.

[S2] T. Umeyama, T. Hanaoka, J. Baek, T. Higashino, F. Abou-Chahine, N. V. Tkachenko and H. Imahori, *J. Phys. Chem. C*, 2016, **120**, 28337.

[S3] K.-Y. Kim, S. Liu, M. E. Köse and K. S. Schanze, *Inorg. Chem.*, 2006, **45**, 2509.

[S4] S. Zhu, L. Wang, B. Li, Y. Song, X. Zhao, G. Zhang, S. Zhang, S. Lu, J. Zhang, H. Wang, H. Sun and B. Yang, *Carbon*, 2014, **77**, 462.

[S5] T. Umeyama, J. Mihara, H. Hayashi, N. Kadota, V. Chukharev, N. V. Tkachenko, H. Lemmetyinen, K. Yoshida, S. Isoda and H. Imahori, *Chem. Commun.*, 2011, **47**, 11781.

[S6] B. E. Hamaoui, F. Laquai, S. Baluschev, J. Wu and K. Müllen, *Synth. Met.*, 2006, **156**, 1182.

[S7] S. K. Das, B. Song, A. Mahler, V. N. Nesterov, A. K. Wilson, O. Ito and F. D’Souza, *J. Phys. Chem. C*, 2014, **118**, 3994.